

Mechanical properties of alumina Nextel™ 720 fibres at room and elevated temperatures: tensile bundle testing

Konstantinos G. Dassios^{a,b,c,*}, Marc Steen^a, Constantina Filiou^a

^a Institute for Energy, Joint Research Centre, European Commission, P.O. Box 2, NL1755 ZG Petten, The Netherlands

^b University of Patras, Department of Mechanical Engineering and Aeronautics, Rio Patras GR-26500, Greece

^c Institute of Chemical Engineering and High Temperature Processes, Foundation of Research and Technology Hellas, Odos Stadiou, Platani, Patras GR-26500, Greece

Received 12 December 2001; received in revised form 22 July 2002

Abstract

Tensile tests on alumina Nextel 720™ fibre bundles were performed and results were analysed using Weibull statistics to calculate the tensile strength and elastic modulus of the fibres as a function of temperature and gauge length. A compliance-correction technique was used to deduce the net fibre strain from the recorded experimental data separately for room and high-temperature tests; the latter tests were performed under inert (argon) gas environments. The Weibull parameters, calculated in terms of strain values, yielded the mean failure strain and the initial compliances yielded the elastic moduli. Both parameters allowed to obtain the mean fibre strength. Statistical analysis was performed to provide a high and low confidence limit for both the Weibull modulus and the strength. Fibre strength was projected to a reference gauge length of 25-mm using the Weibull gauge length correction to allow for comparison with results from single-fibre tests. Room-temperature tests showed that gauge lengths larger than 75 mm are associated with a non-smooth fibre failure regime that can be explained by the larger amount of energy stored in the tested volume at the onset of failure. Results from relevant tests yielded an elastic modulus of 260 GPa and a Weibull modulus of 5.6, 20% less than the value reported by the manufacturer. Fibre strength was substantially less than the value quoted by the manufacturer for both room and high-temperatures; the room-temperature value corresponding to only 53% of the value reported. The observed divergence is a direct effect of the fundamental characteristic of the fibre bundle testing technique which, contrary to the single-fibre test used in the reference studies, is associated with minimal fibre handling and damage and, as such, is believed to fully assess the fibre strength distribution by not eliminating weaker fibres from the population before testing.

© 2002 Elsevier Science B.V. All rights reserved.

Keywords: Alumina fibres; Nextel; Fibre bundle; Weibull; High-temperature testing; Compliance

1. Introduction

Metal oxide ceramics are today one of the primary candidate constituents in the production of composite materials for high-temperature applications. Owing to their inherent oxidation-saturated characteristic, oxide ceramics are chemically stable and have the potential to maintain strength and durability at elevated temperatures, in oxidative and corrosive environments, as for example in aircraft engine parts. Common to all fibre-

reinforced composites, the thermo-mechanical properties of oxide-fibre-reinforced composites depend strongly on those of the reinforcing phase. The statistical strength of the embedded fibres plays a key role in the fracture behaviour of oxide-oxide composites and the parameters that describe their strength distribution have been the topic of various studies.

One of the most renowned ceramic oxide fibres currently available is the alumino-silicate fibre developed by 3M Corporation under the commercial name Nextel™ 720. It is claimed to combine excellent strength with high creep resistance up to 1000 °C. Wilson was the first to test and report the mechanical properties of the Nextel™ 720 fibre. In that study [1], single filaments of a 25 mm gauge length were tested at room and high

* Corresponding author. Tel.: +31-224-565471; fax: +31-224-565636.

E-mail address: dassios@jrc.nl (K.G. Dassios).

temperatures. Using a rubber-faced clamp gripping system, two consecutive test series at room-temperature of approximately 50 single filaments each were performed and the reported statistical strengths of 2130 and 2030 MPa were associated with Weibull moduli of 9.7 and 7.1. Using a second ‘hot grip’ technique intended mainly for high-temperature testing, a room-temperature strength of 1700 MPa was reported. Wilson performed a more dedicated study on the room-temperature mechanical properties of the Nextel™ 720 fibre in 1997, which was exclusively based on single filament tests [2]. The findings of that study are reported by 3M as the mechanical properties of the Nextel™ 720 fibre (Table 1).

Since those first studies, the mechanical properties of the 3M Nextel™ 720 fibre have been extensively re-examined in a number of studies. Goering et al. studied mainly the high-temperature properties of the fibres (creep, thermal stability, subcritical crack growth, role of impurities, microstructural properties) [3,4], but in some of their studies results from room-temperature tests on single filaments are also reported. In [3], 28 fibres of 100 mm gauge length were tested and their mean strength was 1510 MPa whereas the mean strength of 5 fibres of 5 mm gauge length was 2338 MPa. A Weibull modulus of 5.0 was determined by fitting the strength values obtained from the 100 mm gauge length tests to the Weibull distribution. The Weibull modulus based on volume dependence was calculated to be 5.4. In [4], 30 single fibres of 100 mm gauge length confirmed the previous finding for the specific gauge length, whereas 30 monofilaments of 5 mm gauge length provided a new strength value for that gauge length, of 2585 MPa.

In their study on the effect of thermal exposure on the strength of Nextel™ 720 single filaments, Dennis Petry and Mah [5] found the room-temperature mean strength

of 75 sized (as-received) and 76 de-sized fibres of 25.4 mm gauge length to be 1.90 and 1.94 GPa, respectively. Other studies include the single-fibre tests by Das [6] where an unknown number of fibres of 25.4 mm gauge length had a mean strength of 2390 MPa as well as the single-fibre tests of Bunsell et al. [7] where set of 30 filaments were tested at gauge lengths ranging between 5 and 250 mm. Mean tensile strengths of 1.55 ± 0.27 and 1.68 ± 0.39 GPa were reported for 100 and 25 mm gauge lengths, respectively.

The findings of the aforementioned studies, all performed using single-fibre test extracted from Nextel™ 720 tows, have converged to a common value for the Young’s modulus of the fibres at room-temperature of 260 GPa. On the other hand, a significant divergence in the room-temperature mean strength is evident.

Chi et al. pointed out the experimental difficulties associated with the measurement of single-fibre strength to obtain reliable data [8]. Firstly, there is a difficulty in extracting intact individual fibres from a bundle in such quantities that allow for the consideration of a sufficient statistical sample, and the same difficulty applies in testing such fibres of very small diameter. Secondly, and this is common knowledge to scientists who have attempted fibre extractions from a bundle, many fibres fail during the extraction technique. Assuming that a well-rehearsed extraction technique has been established where handling errors can be considered repetitive, any fibres that survive extraction from the bundle can be considered fibres of superior strength, in the same way that the fibres that fail during extraction are the ones that are more prone to damage and fracture, and hence, of lower strength. The single-fibre test can then be considered to truncate the strength distribution towards higher values. The third drawback of the single-fibre technique is associated with the effectiveness of the determination of the cross-sectional area of a single-fibre. In addition to these drawbacks comes the remark that fibres are incorporated in a composite more often as bundles than as single-fibres. It then seems rational that the evaluation of the fibre properties should be performed mainly on fibre bundles, to simulate as closely as possible their behaviour in the real composite.

Fibre bundle testing is a mass-testing technique that overcomes most of the limitations of the single-fibre test and is believed to assess the whole strength distribution of fibres in a bundle. The main advantages of the bundle test are that it involves minimal fibre handling and damage and that it provides a large statistical sample, which is equal to the number of fibres in the bundle (usually of the order of some hundreds). For example, testing a bundle with a filament count of 500 can provide the same information as 500 separate tests on single-fibres. Despite its advantages, the bundle technique has not been widely practised in the case of Nextel™ 720 fibres. Bunsell et al. in a study mainly on Nextel™

Table 1
Properties of Nextel™ 720 fibres (3M Corp.)

Property	Value
Maximum use temperature (°C) (application dependent)	1200
Filament diameter (µm)	10–12
Crystal size (nm)	< 500
Crystal structure	α -Al ₂ O ₃ +3Al ₂ O ₃ ·2SiO ₂ (mullite)
Density (g cm ⁻³)	3.4
Chemical composition (wt%)	85 Al ₂ O ₃ 15 SiO ₂
Thermal expansion (ppm °C ⁻¹) (100–1100 °C)	6.0
Tensile strength (Mpa) (25 mm gauge length)	2100
Tensile modulus (GPa)	260
Creep rate (1 s ⁻¹) (1100 °C/70 MPa)	< 1 × 10 ⁻¹⁰

720 monofilaments, reported tests on bundles at high-temperatures in order to quantify the creep behaviour [9]; unfortunately the measured strengths were not reported in that study.

Based on the above, the following conclusions can be made

- Currently available studies on the room-temperature strength of the Nextel™ 720 fibre report values ranging from 1.6 to 2.4 GPa.
- The reported strengths originate exclusively from single filament tests; the reliability of this technique depends strongly on the method used to extract single fibres from a bundle and can result in biased strength values.
- The fibres are incorporated in a composite as a bundle and it seems more suitable to test them as such.

The combination of the above observations with the authors' experience with mullite-matrix/Nextel™ 720 fibre composites that failed at strengths much lower than expected, gives rise to the need for an accurate re-examination of the Nextel™ 720 mechanical properties using the fibre bundle test to fully determine the single fibre strength distribution.

In the present study, the tensile strength and elastic modulus of Nextel™ 720 are investigated as a function of temperature and gauge length using fibre bundle tests. The high-temperature range chosen in the current study is 600–1200 °C which covers the conventional manufacturing temperature range for composites using this fibre. The upper limit of the temperature range coincides with the maximum use temperature for the fibre, as reported by the manufacturer. The experimental results are analysed using Weibull statistics to deduce the Weibull modulus and mean fibre strength. To compare with reported values, the equivalent fibre strength at a 25 mm gauge length is calculated using the Weibull gauge length correction. A compliance–correction approach is followed to determine the fibre strain from the recorded extension [10]. The findings are compared to the single-fibre results of Wilson [2] (Table 1).

2. Background

2.1. Weakest-link statistics

The Weibull model has been very successful as a life distribution model for the failure mechanism associated with brittle fibres. The strength distribution of the Nextel fibres was analysed following the 2-parameter Weibull distribution function. Under this approach, the survival probability P_s of a single fibre of volume V , up

to a stress σ is given by:

$$P_s(\sigma) = \exp \left[-\frac{V}{V_0} \left(\frac{\sigma}{\sigma_0} \right)^{m_\sigma} \right] \quad (1)$$

where V_0 is a scaling constant, σ_0 is the characteristic fibre strength and m_σ is the Weibull modulus—the index σ indicates it was calculated by means of stress. Assuming a uniform fibre diameter across the fibre length (an assumption whose validity is discussed in a subsequent section), the failure probability P_f of a single fibre at a strain e can be expressed as:

$$P_f(\varepsilon) = 1 - \exp \left[-\frac{L}{L_0} \left(\frac{\varepsilon}{\varepsilon_0} \right)^{m_\varepsilon} \right], \quad (2)$$

where L is the fibre gauge length, L_0 is a reference gauge length (assumed equal to L in this case), ε_0 is the characteristic failure strain and m_ε is the Weibull modulus calculated in terms of strain. Taking twice the natural logarithm of Eq. (2) and rearranging leads to:

$$\ln \ln \frac{1}{1 - P_f(\varepsilon)} = m_\varepsilon \ln \varepsilon - m_\varepsilon \ln \varepsilon_0 \quad (3)$$

The above is a first-order equation between $\ln \ln(1/1 - P_f(\varepsilon))$ and $\ln \varepsilon$ with a slope of m_ε and an ordinate at the intersection with the y -axis of $m_\varepsilon \ln \varepsilon_0$.

Eqs. (1)–(3) hold for single fibres. A fibre bundle consists of a large number of individual fibres which, under the assumption of perfect alignment, act independently. The instance of first fibre failure defines the failure regime whereas, under the global load-sharing principle, each fibre failure is followed by a uniform redistribution of the remaining load to the surviving fibres. Each instance in the failure regime is associated with a distinct failure probability P_f and the probability distribution function can be obtained from a sufficient number of (P_f , e) pairs. The calculation of Weibull parameters based on strain is more efficient than its stress-based counterpart as it does not presuppose knowledge of the number of load-carrying fibres in the bundle.

At each moment during a fibre bundle test, the stress taken up by the bundle, σ_b , can be written as a function of the strain of the bundle, e —which is equal to the strain of the individual fibres—multiplied by the fibres' Young's modulus, E , and their survival probability, P_s :

$$\sigma_b(\varepsilon) = \sigma_{\text{fbr},s}(\varepsilon) P_s(\varepsilon) = \varepsilon E \exp \left[-\left(\frac{\varepsilon}{\varepsilon_0} \right)^{m_\varepsilon} \right] \quad (4)$$

where $\sigma_{\text{fbr},s}(e)$ is the stress on the surviving fibres, a monotonically increasing function of strain.

Once the Weibull parameters and the elastic modulus have been calculated, the empirical Weibull stress–strain approximation, Eq. (4), can be superimposed to the experimental data.

2.2. Weibull gauge length correction

The mean strengths, $\sigma_{\text{mean},1}$ and $\sigma_{\text{mean},2}$ of two otherwise identical fibre bundles (same failure probability, same Weibull parameters) of different gauge lengths, L_1 and L_2 , can be correlated through the Weibull size-effect formula (Eq. (5)) which is useful in projecting the fibre strengths of various gauge lengths to a single gauge length, thus allowing for comparison.

$$\frac{\sigma_{\text{mean},1}}{\sigma_{\text{mean},2}} = \left(\frac{L_2}{L_1} \right)^{\frac{1}{m_e}} \quad (5)$$

3. Experimental

3.1. Materials and specimen preparation

Nextel™ 720 fibre bundles were extracted from a tow supplied by 3M Corporation (lot number A0177-0199). The as-received fibres carried a PVA (poly-vinyl-alcohol) sizing, code number 170, for ease of handling. Experiments with both as-received and de-sized fibres were performed. Removal of the sizing was performed by heat cleaning the fibres in a ventilated furnace at a temperature of 700 °C for 5 min according to the procedure proposed by the manufacturer.

Fibre bundle specimens were prepared according to a new, custom-developed technique: At first, the bundle was optically examined to ensure no initial fibre failure due to handling was contained in the gauge length—if that was true, the bundle was rejected. The bundle was clamped and hung from one end on a vertical preparation rack where it was subsequently straightened by pouring a smooth alcohol flow along their length. After drying, two plastic heat-shrink tubes were fitted with the help of a soldering iron around the fibre bundle at a distance apart equal to the desired gauge length. The remaining (lower) portion of the bundle was inserted into a 75-mm long/6 mm O.D./4 mm I.D. stainless steel tube. The bundle/tube system was rendered one-body by injecting epoxy resin into the tube using a syringe from the bottom to avoid air-bubble entrapment. The other end was prepared similarly with a time interval of 24 h to allow for solidification of the resin. This procedure resulted in specimens with a firm gripping system that enabled indirect load transfer from the grips to the bundle through the resin.

Fifteen specimens intended for room-temperature testing were prepared at gauge lengths of 50, 75, 100 and 140 mm. The specimens were mounted on the mechanical tester using a custom alignment base. The bundle length of the high-temperature specimens was kept constant at 140 mm as dictated by the configura-

tion of the cold-end testing apparatus—the relevant gauge length in the high-temperature tests is the heated length, 20 mm. Both room- and high-temperature tests were performed under extension-control on an Instron hydraulic testing machine equipped with a 25 kN load cell where the cross-head displacement, the reading of the load cell and time were recorded simultaneously. Extension rates varied from 0.084 to 0.5 mm min⁻¹, typical test durations were of the order of 4–10 min for room-temperature tests and 55–70 min for high-temperature tests which included 8–15 min of the heating-up stage, 40 min of residence at the desired temperature and 10–15 min of test time.

3.2. High-temperature testing

A specially designed device was used to perform cold-end high-temperature tests via induction heating in inert gas conditions. Although alumina fibres do not oxidize at high-temperatures, inert environment conditions had to be established to prevent oxidation of the graphite susceptor used to transfer heat to the bundle. The apparatus consists mainly of 4 concentric cylindrical parts that form a multi-layer cylindrical chamber: the susceptor tube, a heat shield surrounding the susceptor (insulating alumina fibrous material), a protective outer cover (Pyrex glass tube) and a water-cooled induction coil. Alloy plates on top and bottom fasten the components together and O-rings are used to assure leak tightness. The covers are equipped with water flow inlets and outlets, an exhaust valve and a thermocouple-fitting aperture. Cold water introduced through the inlets circulates in micro-channels to keep the O-rings of the top and lower covers at safe working temperature. Air that initially resides in the chamber is evacuated and replaced with high-purity argon gas through the evacuation outlet that is connected to an under-/over-pressure system. The specimen is introduced in the chamber from a centric aperture on the top cover so that the bundle is positioned concentric to the susceptor tube. The upper and lower specimen ends are fastened air-tight in place. An induction generator is used to heat the 20 mm long susceptor tube, which, in turn, heats up the central chamber where the bundle resides.

4. Results

4.1. Shape of load–displacement curves

While the elastic regimes of all bundle tests were linear, the load–displacement curves showed deviations from the theoretical Weibull-smooth behaviour in the non-linear region. Primarily, a post-failure ‘tail’ region was apparent in all curves, for an example see Fig. 1. If the end of the failure region is assumed to be the point

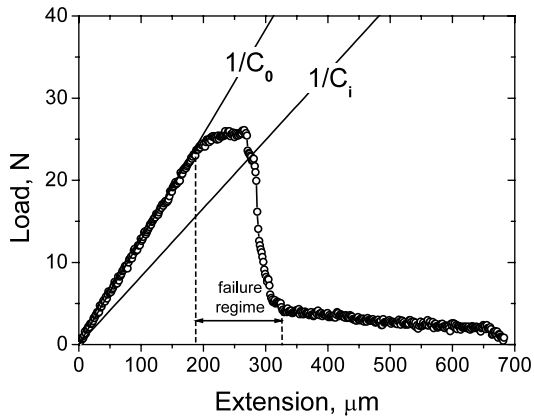


Fig. 1. A typical fibre bundle load–displacement curve. Experimental data are shown as hollow circles whereas the slopes $1/C_0$ and $1/C_i$, corresponding to the elastic and failure regions represent the total initial compliance and the compliance at each failure instance, respectively. The statistical analysis to obtain the Weibull modulus and characteristic failure strain is performed in the failure regime.

where the tangent with negative slope decreases considerably in absolute value, the ‘tail’ behaviour that characterises the post-failure region is an effect of the friction between neighbouring fibres. Since fibres fail at different relative positions inside the tested length, the ‘tail’ effect lasts until that cross-head displacement where the ends of all failed fibres have separated completely. For example, in Fig. 1 the failure region ends at approximately $325 \mu\text{m}$ but load relaxation is achieved only after the cross-head has extended another $350 \mu\text{m}$ where, eventually, all failed fibres in the gauge length have separated. The ‘tail’ region is not considered for the calculation of the Weibull parameters.

Another deviation from the theoretical behaviour was the step-wise decrease in load within the failure region; a phenomenon that is attributed to the ‘dynamic load effect’ associated with fibre failure [8]: When a single fibre in the bundle fails, suddenly the same load has to be shared between the remaining intact fibres, and the portion of load that corresponds to each one of the intact fibres is now greater than before the fibre failure. As a consequence, more fibre failures are induced within a short period of time and thus small step-wise load drops appear in the curves, especially during the last stages of the failure regime where the number of intact fibres is much smaller than in the initial failure stages.

Apart from the dynamic load effect, the recorded failure regions in tests with gauge lengths larger than 75 mm exhibited sudden load drops to zero in the early stages of the failure regime, thus deviating from the theoretically expected Weibull-smooth behaviour. This behaviour is especially evident in larger gauge lengths because of the larger volume that is available for accumulation of energy. From an energetic point of view, after a critical fibre failure occurs at a certain load level, the accumulated energy can be too high for the

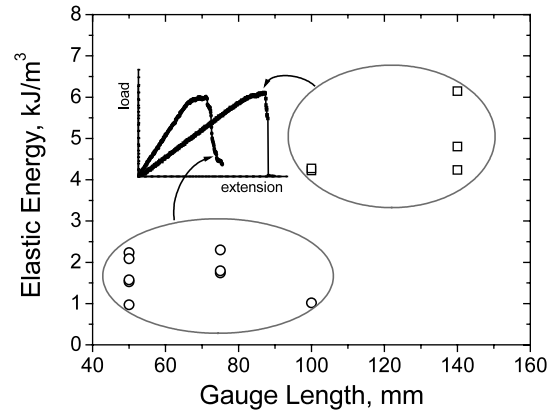


Fig. 2. The amount of elastic energy stored in the fibres in the elastic regime plotted as a function of gauge length. 100 and 140 mm gauge lengths (hollow squares) accumulated a 3–4 times larger amount of energy than 50 and 75 mm gauge lengths (hollow circles). Also shown are the typical load–displacement curves associated with the gauge lengths.

remaining intact fibres to share it evenly as a result of which the rapid failure of the bundle occurs. The higher the energy accumulated in the bundle is, the more drastic its release will be, leading to sharp load/stress drops in bundle tests performed under displacement control. The elastic energy accumulated in the bundle during the loading stages was calculated as the area below the load–displacement curve within the elastic regime and is plotted versus gauge length in Fig. 2. Gauge lengths of 100 and 140 mm accumulated approximately 3–4 times more elastic energy than their 50 and 75 mm counterparts. A consequence of this phenomenon is the extreme value of Weibull modulus obtained for the larger gauge lengths, that is at times triple or quadruple that of the shorter gauge length value (see also Fig. 7). The use of Weibull statistics is clearly not appropriate in such cases because the assumption of global load sharing between non-interacting fibres collapses, and the obtained Weibull parameters (m_e , e_0) are not reliable. In this study, five bundle tests at gauge lengths of 100 and 140 mm exhibited steep failure behaviour. The results of these tests were not considered for calculating the mean Weibull modulus and strength of the fibres.

4.2. Compliance

As direct extensometry cannot be performed on the bundle the total recorded extension has to be corrected for (i) parasitic contributions related to system/set-up inaccuracies (cross-head movement, gripping inaccuracies, etc) for the room-temperature tests as well as (ii) contributions of the different temperature zones present along the specimen in high-temperature tests. The correction was achieved by means of quantifying and subtracting the non-gauge length compliance from the

total compliance, as described in the following. In a series of room-temperature tests with different gauge lengths, the compliance of the elastic region, ‘initial compliance’, C_0 , is evaluated and plotted as a function of gauge length. The resultant linear plot is extrapolated to a zero gauge length to obtain the extension per unit load as if no sample were present and only parasitic extensions were to be recorded. This parasitic or system compliance, C_p , is defined as the ordinate of the intersection point of the linear plot with the y -axis. For room-temperature testing, the parasitic compliance is subtracted from the total instantaneous compliance, (C_0 for the elastic region and C_i for the failure region), to obtain the net bundle compliance. C_0 and C_i are defined graphically in Fig. 1, whereas the determination of the parasitic compliance is presented graphically in Fig. 3. With only the fibre bundle gauge length changing, the parasitic compliance, C_p , is assumed to remain constant during a series of tests.

In high-temperature cold-end tests, the total recorded extension incorporates not only parasitic contributions due to the experimental setup but also contributions from all three temperature zones present along the length of the specimen: the heated zone, the temperature gradient zone and the cold zone. Each one of the temperature zones is associated with a different compliance (C_h , C_g and C_c , respectively). Only the heated zone compliance is relevant for the test result and contributions from the remaining zones have to be subtracted from the total extension. In high-temperature cold-end testing the heated length remains constant while the total length changes, thus the compliances of the heated zone and the gradient zone remain constant and only the cold zone compliance changes. For a small gradient zone, C_g can be neglected [10] and the sum $C_h + C_p$ can be found by extrapolating the total com-

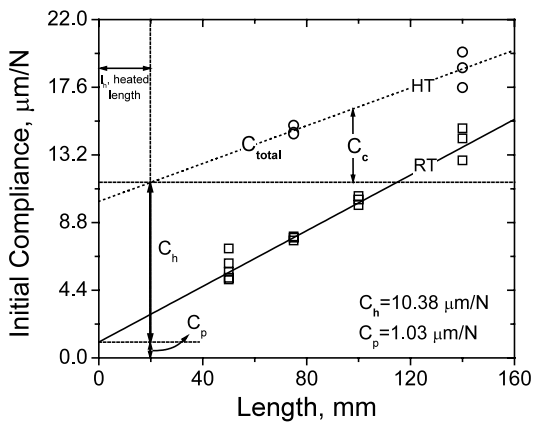


Fig. 3. Calculation of the parasitic compliance C_p at room-temperature (hollow square symbols) and the hot-zone compliance C_h of high-temperature tests (hollow circle symbols). The symbols represent the inverse of initial slopes of the load–displacement curves of fibre bundle tests. The high-temperature data correspond to temperatures of 600, 800 and 1000 °C.

pliance to the heated length, l_h , where also the cold zone compliance, C_c , is by definition zero (Fig. 3).

4.3. Statistical analysis

The elastic modulus as well as fibre strain/failure probability pairs associated with each failure instance, are evaluated separately for each bundle test according to the equations presented in Table 2, following the method presented in CEN ENV 1007-5 standard [11]. In Table 2, F_i is the instantaneous load, l_h is the heated length (20 mm) and A_0 is the initial cross-sectional area of a bundle with a initial population of N_0 load-carrying fibres with a diameter of D_f . A_0 is calculated following Eq. (12).

$$A_0 = N_0 \pi \frac{D_f^2}{4} \quad (12)$$

The pairs $(P_{f,i}, e_i)$, as calculated from Eqs. (6)–(9), are fitted to Eq. (3) to calculate the Weibull parameters m_e and e_0 . Upper and lower limits for the Weibull modulus and characteristic failure strain were evaluated for a 90% confidence level following the procedure proposed in CEN ENV 843/5 [12]. The mean failure strain, e_{mean} , is calculated from the characteristic failure strain, e_0 through:

$$e_{\text{mean}} = \frac{e_0}{\Gamma\left(1 + \frac{1}{m_e}\right)} \quad (13)$$

where Γ is the gamma function. The mean strength, σ_{mean} , of the fibres in the tested bundle is calculated as the product of the mean failure strain and the elastic modulus after Eqs. (10), (11) and (13). The equivalent mean fibre strength at a 25 mm gauge length, $\sigma_{\text{mean},25}$, is evaluated through Eq. (5) for L_1 equal to the tested gauge length and $L_2 = 25$ mm. The upper and lower limits of the mean fibre strength at 25 mm were calculated as a product of the corresponding e_0 limits with the elastic modulus.

The Weibull stress–strain regression is derived after introduction of the calculated Weibull parameters and

Table 2
Calculation of probability and strain distribution in room- and high-temperature tests

	RT	HT
Fibre failure probability, $P_{f,i}$ ^a	$\frac{C_i - C_0}{C_i - C_p}$	$\frac{C_i - C_0}{C_i - (C_h + C_p)}$
Fibre strain, e_i ^a	$\frac{(C_i - C_p)F_i}{L_0}$	$\frac{[C_i - (C_h + C_p)]F_i}{l_h}$
Young's modulus, E	$\frac{L_0}{A_0}(C_0 - C_p)^{-1}$	$\frac{l_h}{A_0}[C_0 - (C_h + C_p)]^{-1}$

^a Used in the Weibull statistical analysis.

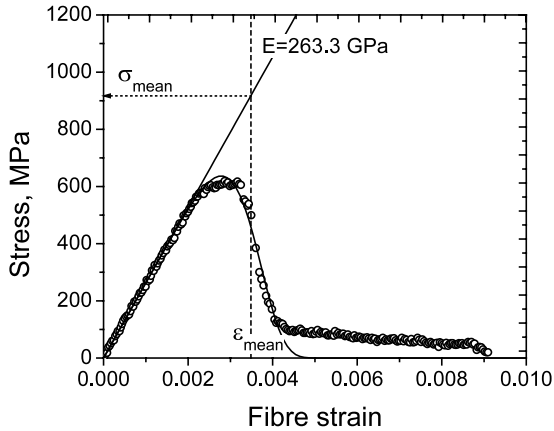


Fig. 4. The fibre bundle stress–strain curve (hollow circles) of Fig. 1 plotted together with the Weibull regression (Eq. (4)). The fit shows good agreement in the failure regime. See text for a brief explanation of the ‘tail’ behaviour. Also shown are the elastic modulus, the mean failure strain ($\epsilon_{\text{mean}} = 0.0034$) and the mean failure stress of 904 MPa at the intersection point of E and ϵ_{mean} .

elastic modulus in Eq. (4); a typical resultant curve is presented in Fig. 4 for a 75 mm gauge length tested at room-temperature. The Weibull plots of the room and high-temperature tests are summarized in Fig. 5 whereas Fig. 6 illustrates the effect of temperature on the elastic modulus and strength of the fibres. A summary of all results is given in Table 3. At room-temperature, the Weibull modulus and the mean fibre strength—normalized to a reference gauge length of 25 mm—are the arithmetic averages from 10 relevant tests. The room-temperature elastic modulus is the arithmetic average of all 15 tests.

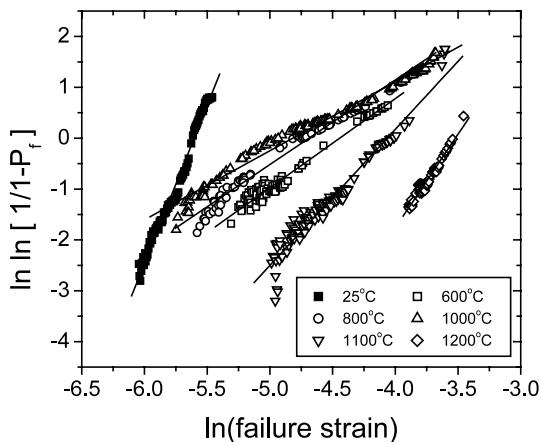


Fig. 5. Weibull plots for the 600, 800, 1000, 1100 and 1200 °C fibre bundle tests with a gauge (heated) length of 20 mm. Also shown is the typical Weibull plot of the 75 mm room-temperature test (Fig. 4) with the significantly steeper slope (larger Weibull modulus) that is directly associated with the narrower failure strain distribution of the room-temperature tests.

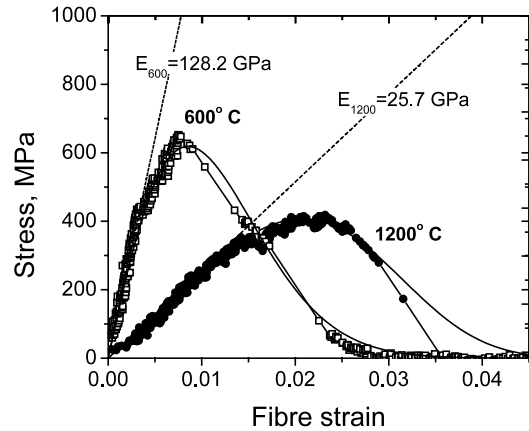


Fig. 6. Experimental stress–strain curves of fibre bundle tests at 600 °C (hollow squares) and 1200 °C (solid circles) plotted together with the Weibull regressions (straight lines). The curves demonstrate the degradation of strength and elastic modulus with temperature.

5. Discussion

5.1. Room temperature—comparison with reported values

The room-temperature elastic modulus (Table 3) compares favourably with the value reported by the manufacturer (260 GPa, Table 1). This also provides evidence that almost all the fibres in the bundle are load-bearing. The average value of the room-temperature Weibull modulus, 5.6, is 25% less than the corresponding single-fibre value, 7.6 [2] whereas the 90% confidence limits for the Weibull modulus are 4.5 and 6.7. The Weibull modulus is plotted against gauge length in Fig. 7. No relation between the gauge length and the Weibull moduli from relevant tests results can be noted. The gauge length-dependence of the room-temperature tensile strength is shown in Fig. 8. By extrapolating the linear fit (of the relevant results) to a gauge length of 25 mm, a strength value of 1213 MPa is obtained which compares well with the mean strength of 1117 MPa (Table 3) calculated through the Weibull gauge length correction (Eq. (5)). However, the room-temperature fibre strength is only 53% of the value reported by the manufacturer, 2100 MPa ([2,13]). The latter was the average strength of 50 single-fibre tests at 25 mm gauge length; the absolute values ranged between 1500 and 2700 MPa with a standard deviation of 287 MPa. The standard deviation associated with the mean room-temperature strength calculated in this study is significantly lower, 163 MPa, a fact that may also be attributed to the larger number of the statistical sample of the present study (10 fibre bundles of approximately 360 individual fibres each as compared to 50 single-fibre tests). In the following, a rationalization of the observed divergence from the single-fibre test is attempted.

Table 3
Summary of results

Temperature (°C)	m_e		E (GPa)	$\sigma_{\text{mean},25}$ (MPa)	
	Mean value	90% Confidence range		Average value	90% Confidence range
25	5.6	4.5–6.7	257.7	1117	1053–1188
	10 relevant tests		15 tests	10 relevant tests	
600	1.7		128.2	1182	
800	1.6		146.1	1050	
1000	1.3		151.1	950	
1100	2.6		54.6	767	
1200	3.6		25.7	646	

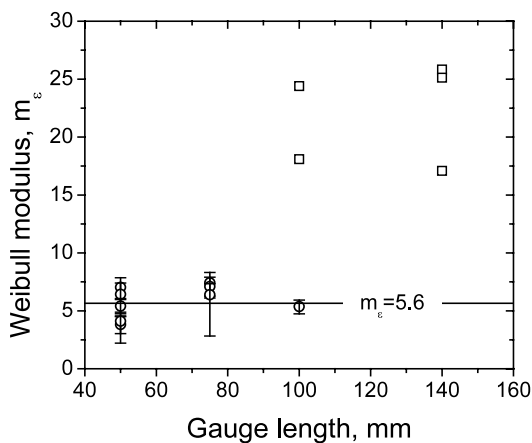


Fig. 7. The Weibull modulus, m_e , plotted versus gauge length. The straight line is the mean value of the Weibull modulus. Open squares correspond to tests that exhibited sudden load drops and are not included in the calculation of the mean Weibull modulus. Wider limits are a result of fewer available data in the failure regime.

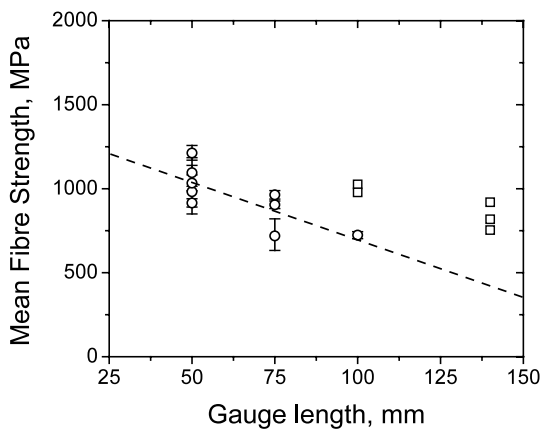


Fig. 8. The room-temperature tensile strength of fibres plotted as a function of gauge length. Open circles represent results from relevant tests that exhibited smooth failure regimes whereas open squares are strengths of untrusted larger gauge length tests that failed suddenly and do not contribute in the strength statistics. Also shown are the upper and lower limits of the relevant strengths at a 90% confidence level. The dashed line is the linear fit to the relevant strength results.

The load transfer efficiency of the gripping system is examined first. In all experiments, bundle failure occurred in the middle part of the tested gauge length and no defects were noted near the gripping ends where problems with load transfer would have been evident as fibre failure or pull-out. Thus, the cold-end gripping system used in the current study is believed to be firm and to efficiently enable load transfer to the bundle—and the fibres within—via the epoxy resin.

The mean fibre strength is calculated as the product of mean failure strain with elastic modulus; the latter quantity incorporates the bundle cross-sectional area (Eq. (10)) and, hence, the number and diameter of fibres. Firstly, optical microscope examination was performed to estimate the number of load-carrying fibres in the bundle as well as to measure their diameter. Four samples—one of each gauge length tested at room-temperature—were prepared by removing a slice of the tubular gripping end of the specimens where the fibres were embedded in the epoxy resin. The samples were subsequently polished to enable fine imaging of the cross-sectional area. The number of fibres present in the examined cross-sections was 357 (mean value); this value is within 85% of the ‘nominal filament count’, 420, that was stated on the bundle tow label and was used in the calculation of the fibre bundle cross-sectional area (Eq. (12)). A hypothetical reconciliation of this quantity so that the strength product would be equal to the reported value, leads to the finding that approximately only half of the fibres in the bundle should actually be load-carrying, a scenario which can be excluded as pre-test optical examination of the tested bundles showed all fibres in the volume to be intact. An additional reason that supports the allegation that the number of load-carrying fibres is not responsible for the low fibre strength calculated is the value of the calculated elastic modulus. The number of fibres appears in the calculation of the elastic modulus (Table 2); if the number of fibres were smaller, the calculated modulus would not have been similar to the reported value. Additionally, imaging analysis software was used to measure 100 fibre diameters that were found to vary around a mean value

of 12.24 μm with a standard deviation of 0.50 μm . The corresponding coefficient of variation, 4.0%, validated the diameter value used in the calculations (12.2 μm) as well as the assumption adopted in this analysis, that fibre diameter can be considered uniform throughout the bundle cross-section.

Accepting that the fibre strength calculated in this study is not affected by the efficiency of load transfer to the bundle nor by the value of the bundle cross-sectional area used in the analysis, the observed divergence may be explained by the superior strength of individual fibres tested in the single-fibre test. This does not mean that the spool from which the bundles were extracted for this study was of inferior strength due to manufacturing/production details. Instead it suggests that the procedure for extracting individual fibres from the bundle for the single-fibre test biases the strength of the tested fibres-in contrast to a fibre bundle test where fibres undergo minimal handling. If a fibre can survive manual extraction from a bundle, it can be considered to be one of the stronger fibres by origin. Moreover, the proportionality between strong and weak fibres in a bundle affects the shape, m_e , and location, e_0 , of the distribution. This remark has been extensively discussed by Chi et al [8] and Phani [14] and is of particular importance especially for the case of alumina fibres that are extremely brittle. In that sense, testing fibres extracted from a bundle can be considered a test on superior-strength fibres. The mass testing technique followed in this study is believed to overcome this inherent limitation of the single-fibre test.

5.2. High-temperature

Results of tests at high-temperatures showed a degradation of the fibre mechanical properties with increasing temperature, Fig. 9. The strengths of fibres tested at 600 and 800 $^{\circ}\text{C}$ remained within 90% of the

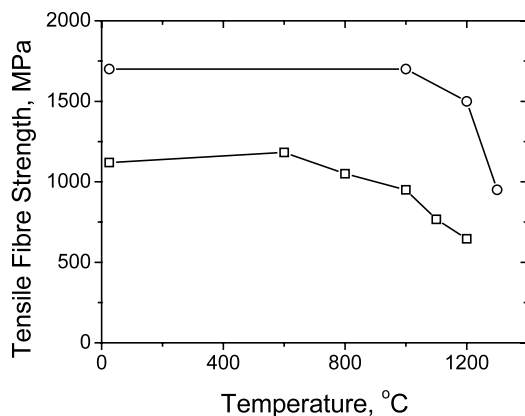


Fig. 9. The mean tensile strength of Nextel™ 720 fibres (projected to a 25 mm gauge length) as a function of temperature. Square and circle symbols represent results from this study and the reference work by Wilson et al. [5], respectively.

room-temperature value. Qualitatively, the fact that the strength degradation and creep of the Nextel™ 720 fibres commences at approximately 1000 $^{\circ}\text{C}$ is in agreement with other studies [1]. At 1200 $^{\circ}\text{C}$ the fibre strength has dropped to 42% of the room temperature value (1117 MPa \rightarrow 646 MPa), compared to the finding of 12% drop (1700 MPa \rightarrow 1500 MPa) by Wilson et al [1]. The elastic modulus decreased to 50% of the room-temperature value at 600 $^{\circ}\text{C}$ and reached 10% of the room-temperature value at 1200 $^{\circ}\text{C}$.

5.3. Design implications

The Weibull modulus and strength of fibres have special relevance in the fracture behaviour of continuous-fibre ceramic composite materials where the mechanical properties of the reinforcing phase are known to play a dominant role in the structural integrity of the material after first-matrix cracking. Ideally, fibres used in composite materials must combine high strength with a fairly wide strength distribution. The excellent combination of height and width of the Nextel™ 720 strength distribution in conjunction with its oxide characteristic make it an ideal candidate for use in composite materials targeted for applications at high-temperature oxidative environments.

6. Conclusions

Tensile bundle testing was performed on alumina Nextel™ 720 fibres under both room- and high-temperature inert-gas environments and the tensile strength projected to a reference gauge length of 25 mm equals 1117 MPa at room-temperature and 646 MPa at 1200 $^{\circ}\text{C}$. The room-temperature strength value corresponds to only half the value obtained from a series of single-fibre tests whereas the rate of decrease of strength with temperature agrees with bibliography. After eliminating various factors that could be responsible for the noted discrepancy, it is concluded that the fibre bundle testing technique is more efficient in assessing the fibre strength distribution than the single-fibre test which leaves only the stronger fibres for testing, and results in an artificial truncation of the strength distribution combined with an apparent increase in fibre strength and Weibull modulus. During this study it was noted that gauge lengths greater than 75 mm tested at room-temperature exhibited very steep failure regimes as a result of accumulation of higher amounts of elastic energy; thus precluding the use of Weibull statistics for these gauge lengths.

Acknowledgements

The valuable guidance of Stefan Ripplinger in specimen preparation as well as in the technical part of high temperature testing is gratefully appreciated. In addition, the experienced assistance of Burkhard Fisher in many experimental details of this study is thankfully acknowledged. This study has been performed within the R&D programme of the European Commission. The authors also wish to thank Prof. Vassilis Kostopoulos of the Department of Mechanical Engineering and Aeronautics, University of Patras, Greece and Research Director Dr Costas Galiotis of the Institute of Chemical Engineering and High Temperature Processes, Foundation for Research and Technology, Hellas for their input and support throughout this study.

References

- [1] D.M. Wilson, S.L. Lieder, D.C. Lueneburg, Proceeding of the 19th Annual Conference on Composites, Advanced Ceramics, Materials and Structures—B, Ceramic Engineering and Science Proceedings 15 (5) (1995) 1005.
- [2] D.M. Wilson, *Journal of Materials Science* 32 (1997) 2535.
- [3] J. Goering, H. Schneider, Creep and Subcritical Crack Growth of Nextel 720 Alumino Silicate Fibres As Received and After Heat Treatment at 1300 °C, Proceeding of the 21st Annual Conference on Composites, Advanced Ceramics, Materials and Structures—A, Ceramic Engineering and Science Proceedings 18 (3) (1997) 95.
- [4] H. Schneider, J. Goering, M. Schmeucker, F. Flucht, Thermal Stability of Nextel 720 Alumino Silicate Fibers, Ceramic Microstructure: Control at the Atomic Level Edited by A.P. Tomsia and A. Glaeser New York (1998), 721.
- [5] M. Dennis Petry, T.I. Mah, *Journal of American Ceramic Society* 82 (10) (1999) 2801.
- [6] Gopal Das, Thermal Stability of Single Fibre and Polycrystalline Alumina Fibres and 85% Al₂O₃–15% SiO₂ Fibers, Proceeding of the 19th Annual Conference on Composites, Advanced Ceramics, Materials and Structures—B, Ceramic Engineering and Science Proceedings 15 (5) (1995) 977.
- [7] F. Deleglise, M.H. Berger, D. Jeulin, A.R. Bunsell, *Journal of the European Ceramic Society* 21 (2001) 569.
- [8] Zhifan Chi, Tsu-Wei Chou, Guoyi Shen, *Journal of Materials Science* 19 (1984) 3319.
- [9] F. Deleglise, M.H. Berger, A.R. Bunsell, Microstructural Evolution and Mechanical Behaviour up to 1500 °C of Nextel 720 Mullite-Alumina Fibres, Proceedings of the Fourth International Conference on High Temperature Ceramic Matrix Composites (HT-CMC 4), October 2001, Munich, Germany, 84.
- [10] R. Paar, P. Bonnel, M. Steen, *Advanced Composites Letters* 7 (3) (1998) 69.
- [11] ENV 1007-5 Céramiques Techniques Avancées—Céramiques Composites—Méthodes D'essais Pour Les Renforts-Partie 5: Détermination Des Distributions Des Resistances A Rupture Des Filaments Dans Un Fil E Temperature Ambiante.
- [12] ENV 843/5 Advanced Monolithic Ceramic—Mechanical Tests at Room Temperature—Statistical Analysis.
- [13] 3M Nextel™ Ceramic Fibre Technical Notebook, 3M Ceramic Fiber Products.
- [14] K.K. Phani, *Journal of Materials Science* 23 (1988) 941.